Synergistic Effect of Hydrogen Bonds and Chemical Bonds to Construct a Starch-Based Water-Absorbing/Retaining Hydrogel Composite Reinforced with Cellulose and Poly(ethylene glycol)

Longfei Gao, Huiyuan Luo, Qian Wang, Guirong Hu, and Yuzhu Xiong*

ACCESS | Metrics & More | Article Recommendations

ABSTRACT: The hydrogel prepared by graft copolymerization of starch (ST) and acrylamide (AM) is a commonly used absorbent material; however, due to their irregular network structure and a limited number of hydrophilic groups, starch-based hydrogels have poor water absorption and water retention. To overcome this, here, we provide a new preparation method for starch-based hydrogels. Using cerium ammonium nitrate (CAN) as an initiator, the starch−acrylamide−cellulose (CMC)/poly(ethylene glycol) (S-A-M/PEG) superabsorbent hydrogel was prepared by graft copolymerization. The starch−acrylamide−cellulose/poly(ethylene glycol) hydrogel network is constructed through the synergistic effect of hydrogen bonds and chemical bonds. The experimental results showed that the starch−acrylamide−cellulose/poly(ethylene glycol) superabsorbent hydrogel has a complete network structure that does not easily collapse due to its superior mechanical properties. The water swelling rate reached 80.24 times, and it reached 50.61% water retention after 16 days. This hydrogel has excellent water-absorbing and water-retaining properties, biocompatibility, and degradability, making it useful for further studies in medical, agricultural, and other fields.
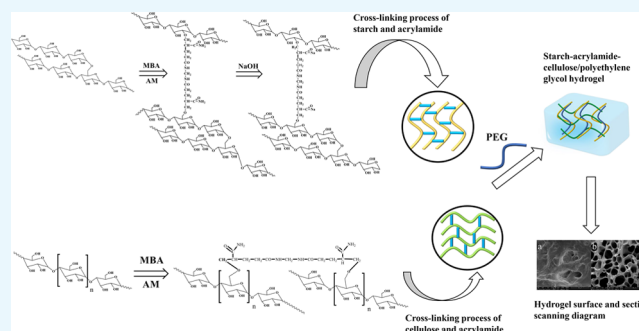
1. INTRODUCTION

Water is the most important resource for human societies, but due to global warming, indiscriminate cutting has caused soil erosion and industrial pollution, resulting in a serious shortage of global freshwater resources. This has also introduced serious global desertification problems.[1] The development of super-absorbent and water-retaining materials for deserts is an important method for solving soil erosion and increasing the survival rate of vegetation.[2−5]

Hydrogels are high-molecular-weight polymers whose unique three-dimensional network structure endows them with good water absorption capacities.[6] A superabsorbent hydrogel can absorb and store large amounts of water Their excellent water retention performance and slow release of water make them widely used in agriculture and horticulture. In areas where water resources are scarce, superabsorbent hydrogels can help reduce the use of irrigation water by maintaining soil moisture. Studies have shown that super-absorbent hydrogels can regulate the evaporation and infiltration of water by affecting the density and structure of the soil, which improves the nutrient retention and physical properties of the soil.[7] These unique water-absorbing materials can also inhibit soil compaction by reducing the frequency of irrigation and preventing soil erosion. Their role in improving microbial activity can bring great benefits to agricultural

production.[8] Superabsorbent gels are mainly divided into two categories, including natural polymer hydrogels and synthetic superabsorbent gels. The main matrix materials of traditional synthetic superabsorbent hydrogels are acrylic and acrylamide polymers.[9] Although these materials are widely used in agriculture and many other industries due to their good water absorption properties and mechanical strength,[10] they have poor degradation properties,[11] which can lead to white pollution. To solve these problems and improve the utilization of superabsorbent gels, researchers have developed various natural biological materials as the matrix materials of superabsorbent hydrogels, which mainly include sodium alginate, gelatin, cellulose, chitosan, and starch.[12−15] Super-absorbent gels prepared using such natural polymeric materials have good water absorption and retention properties and do not cause problems such as soil compaction when they degrade.[16]
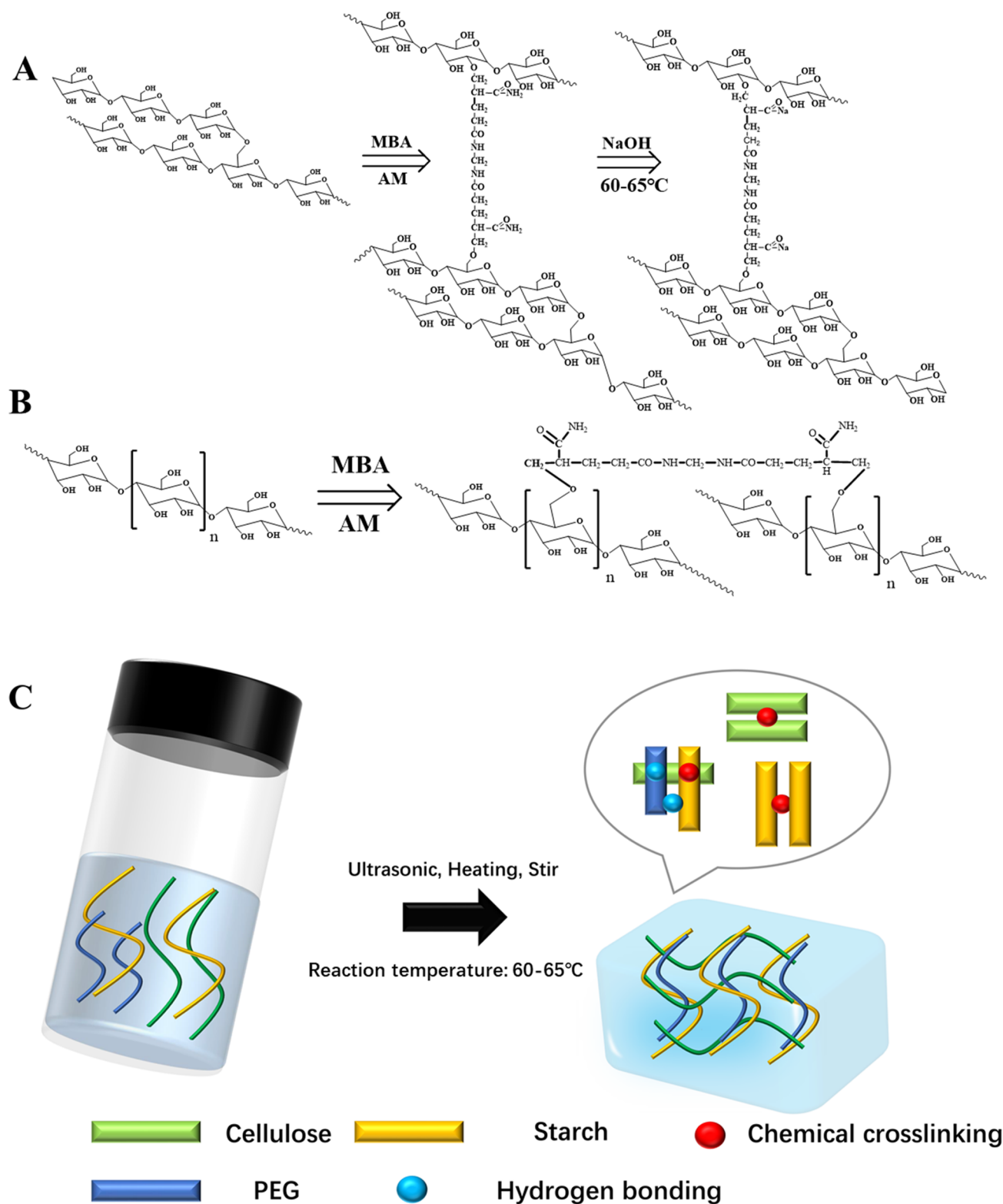
Figure 1. Process of starch cross-linking with acrylamide (A). The cross-linking process of cellulose and acrylamide (B). The proposed reaction mechanism for the superabsorbent composite (C).

Starch and cellulose are the most common polysaccharide materials in nature. They have many advantages such as biodegradability, good stability, safety and nontoxicity, environmental friendliness, wide sources, renewability, and low price.[17−20] They are widely used to prepare degradable water-absorbent gels. For example, superabsorbent materials

prepared using cellulose as a matrix fall into two main categories. One is superabsorbent gels prepared by the grafting of cellulose and acrylic materials.[21] The other type of gel is prepared from cellulose derivatives such as carboxymethyl cellulose.[22] Similar to cellulose, starch is also widely used to prepare superabsorbent hydrogels due to its abundant raw
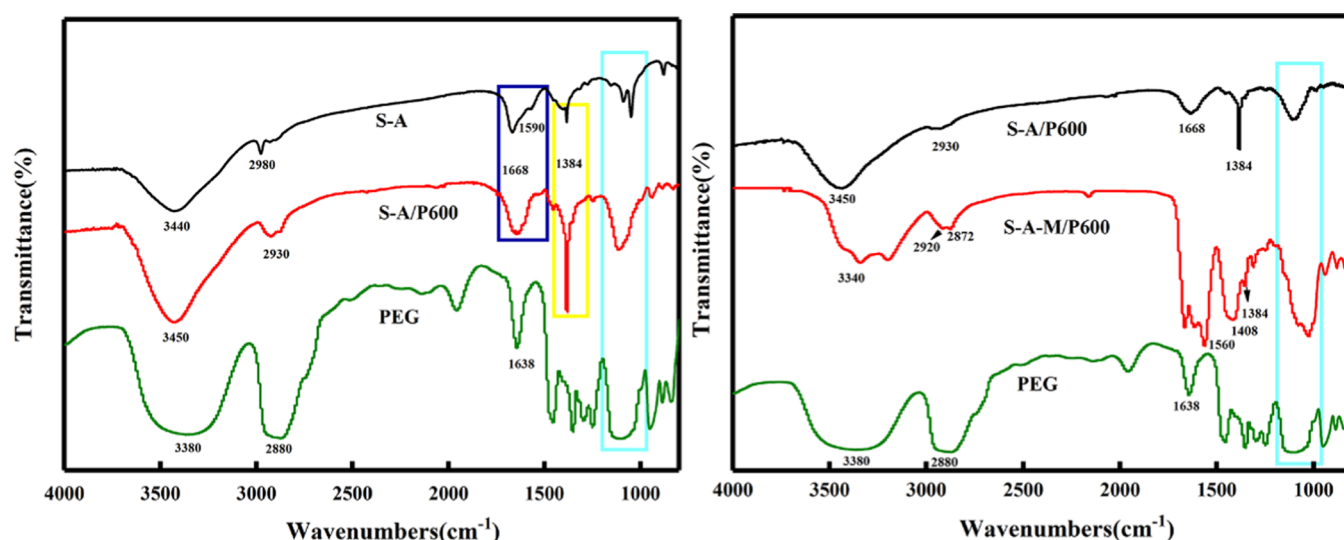
Figure 2. FTIR spectra of S-A, S-A/P600, S-A-M/P600, and PEG.

materials, low price, good biocompatibility, and degradability. Zhang et al.[23] synthesized two superabsorbent hydrogels by the solution-based graft copolymerization of acrylic acid and acrylamide.

Starch-based hydrogels are widely used in many fields such as medicine, health, engineering, agriculture, forestry, and horticulture due to their many advantages.[24−28]

However, compared with the general chemically synthesized hydrogels, natural polysaccharide materials often have the disadvantage of weaker mechanical properties. To better improve the mechanical properties of polysaccharide-based hydrogels, a combination of physical and chemical cross-linking has become a very important approach.[29] To combine the various advantages of cellulose, starch, and acrylic materials, based on the scientific theoretical basis of polymer materials and renewable resource recycling technology, egulating the structure−performance relationship of materials at the molecular level, designing starch−acrylamide−cellulose composite hydrogels with ideal microstructures, excellent water absorption and water retention, and good mechanical properties have become a focus of recent absorbent gel preparation research.

In this paper, starch, cellulose, and acrylamide were used as the matrix materials to prepare starch−acrylamide−cellulose/poly(ethylene glycol) hydrogels (S-A-M/P600) with high water retention and water absorption. The hydrogel was prepared by the graft copolymerization of starch, cellulose, and acrylamide. The influence of adding poly(ethylene glycol) (PEG) with different molecular weights on the water absorption and water retention of the starch-based hydrogels was discussed. The hydrogen bonds between poly(ethylene glycol), starch molecular chains, and cellulose molecular chains produced a synergistic effect with the chemical bonds between starch, cellulose, and acrylamide. At the same time, the rigid cellulose molecular chain is added to solve the problems of network structure collapse and insufficient mechanical strength caused by the addition of flexible poly(ethylene glycol). The hydrogel prepared under these two conditions displayed a regular network structure that did not easily collapse, which greatly improved its water absorption and retention. The experimental results show that through the synergistic effect of chemical and physical cross-linking, our prepared hydrogels

possess excellent water absorption and retention properties, degradability, and biocompatibility while solving the disadvantage of weak mechanical properties of biohydrogels.[30] This paper provides a new idea for the preparation of a new type of superabsorbent and water-retaining hydrogel.

2. RESULTS AND DISCUSSION

2.1. Synthesis Mechanism. The grafting reaction between starch and acrylamide is shown in Figure 1A. The starch gelatinizes under the action of moisture and shear forces, which destroys the hydrogen bonds between starch. The pasting temperature of starch occurs at 60−65 °C. Only when the pasting temperature is reached, the macromolecular chain of starch can be completely opened and the semicrystalline structure of starch can be destroyed so that the grafting reaction with acrylamide can occur and the network structure can be formed.[31] Starch and acrylamide were mixed uniformly under ultrasonic and mechanical stirring. In the presence of an initiator, free radicals were generated on the starch molecular chain, which reacted with the double bond of acrylamide. To improve the water absorption capacity of the hydrogel, a sodium hydroxide solution was added during the final stage of the reaction. At a high temperature, NaOH can convert the amide groups ($-CO-NH_2$) on the polyacrylamide side chains into a more hydrophilic carboxylate ($-COONa$) group.[32] The reaction temperature is 65 °C; only when the reaction temperature is reached, the molecular chain of starch can produce free radicals under the action of the initiator, thus reacting with the double bond of acrylamide. Otherwise, there is no way for the grafting reaction to occur.[33] The initiator CAN can directly react with the starch in a redox reaction to produce starch macromolecule radicals, and this reaction has a high initiation efficiency.[34] The grafting reaction between cellulose and acrylamide is shown in Figure 1B. Under the action of the initiator, the hydroxyl groups on the cellulose side chain generate free radicals; the double bond of acrylamide is grafted with the hydroxyl group in cellulose.

The abovementioned two molecular chains were continuously mixed uniformly under the action of ultrasonication and mechanical stirring. Poly(ethylene glycol) was added, which formed hydrogen bonds with the two molecular chains. Finally, under the synergistic action of hydrogen bonds and chemical
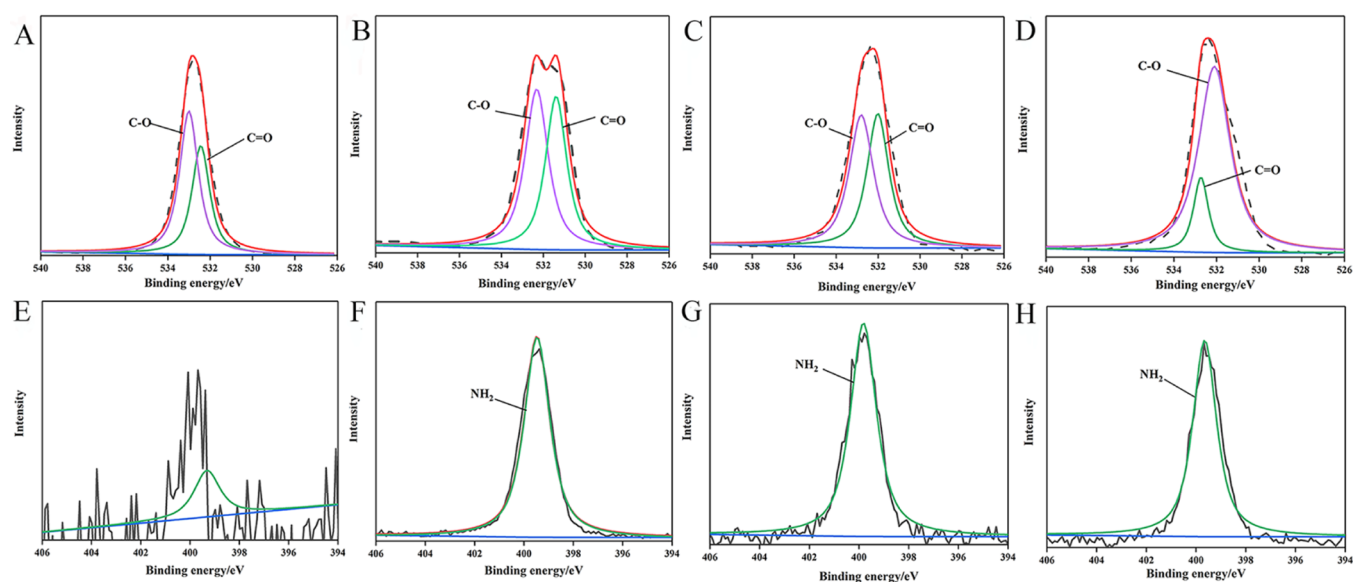
Figure 3. XPS profiles of O 1s and N 1s in MS (A, E), S-A (B, F), S-A/600 (C, G), and S-A-M/600 (D, H).
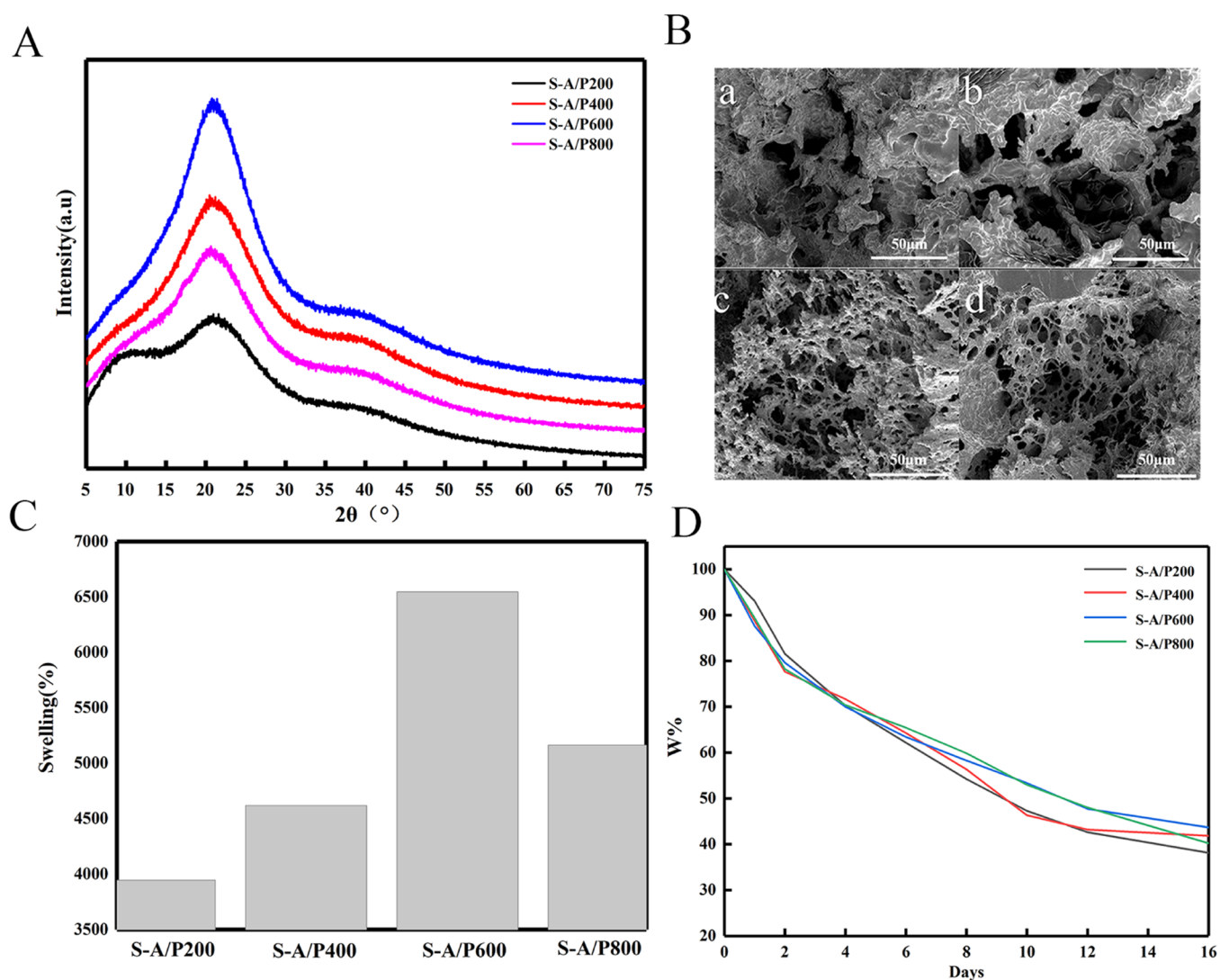

Figure 4. XRD image of starch−acrylamide/poly(ethylene glycol) hydrogel (A), SEM image of starch−acrylamide/poly(ethylene glycol) hydrogel (B), swelling performance of starch−acrylamide/poly(ethylene glycol) hydrogel (C), and water retention performance of starch−acrylamide/ poly(ethylene glycol) hydrogel (D).

bonds, a three-dimensional network structure of hydrogels is constructed.

2.2. FTIR Analysis (Fourier Infrared Spectroscopy) and XPS Analysis (X-ray Photoelectron Spectroscopy).

Figure 2 shows the FTIR spectra of the starch acrylamide hydrogel (S-A), starch−acrylamide/poly(ethylene glycol) hydrogel (S-A/P600), starch−acrylamide−cellulose poly-(ethylene glycol) hydrogel (S-A-M/P600), and poly(ethylene glycol) (PEG). The infrared spectra of S-A, S-A/P600, and S-A-M/600 contain an absorption peak at 1560 cm^{-1} that is caused by the superposition of the 1668 cm^{-1} stretching vibration peak generated by C=O on the amide and the bending vibration peak of the NH group of the primary amide. The peak at 1384 cm^{-1} was produced by the CN stretching vibration. The presence of these absorption peaks indicates that acrylamide was successfully grafted to the starch and cellulose molecular chain.[35,36] In the infrared spectra of S-A/P600 and S-A-M/P600, the obvious enhancement in the peak at 1384 cm^{-1} indicates that the stretching vibration of the C−N bond was strengthened. This indicates that the addition of poly(ethylene glycol) significantly increased the grafting rate of acrylamide and starch. In the infrared spectra of the three hydrogels, the stretching vibration peaks of the methylene group on the glucose unit still existed at 2980 and 2930 cm^{-1}, indicating that the backbone of the starch molecule was not changed. In the S-A/P600 infrared spectrum, after adding PEG, no new peak was formed, which indicates that PEG was only physically blended and no grafting reaction occurred during the gel formation process. The −OH peak at 3450 cm^{-1} shifted to a higher wavenumber, which indicates strong hydrogen bonds between poly(ethylene glycol) and starch grafted groups.[37] In the infrared spectrum of S-A-M/P600, strong absorption bands were observed at 2920 and 2872 cm^{-1} due to the overlapping effect of C−H stretching of cellulose and acrylamide.[38] There are two absorption vibration peaks at 1560 and 1408 cm^{-1}, which can indicate that acrylamide was grafted onto the cellulose molecular chain.[39] Figure 3 shows the XPS patterns of starch and the three hydrogels. The O 1s consists of two fitted peaks for O=C and O−C, centered at 532.48, 532.98 eV. However, no peaks were evident in the N 1s, and there appeared to be no nitrogen in the sample. For S-A, it mainly contains C, O, and N elements; the nitrogen element mainly comes from acrylamide. O 1s consists of two fitted peaks of O=C and O−C, respectively, centered at 532.35 and 531.42 eV. For S-A/P600, O 1s consisted of two fitted peaks of C=O and C−O centered at 532.78 and 531.98 eV, respectively. The O 1s binding energy group of S-A/P600 was slightly altered due to the formation of hydrogen bonding interaction between poly(ethylene glycol) and starch, which can change the O 1s binding energy of the C=O and C−O group. This coincides with the hydrogen bonding peak produced in the infrared spectroscopy analysis.[40]

As for S-A-M/P600, it also mainly contains C, O, and N elements; the nitrogen element mainly comes from acrylamide. O 1s consists of two fitted peaks of O=C and O−C, respectively, centered at 532.08 and 532.68 eV. Since the cross-linking reaction between cellulose and acrylamide also occurred, which led to a great change in the chemical environment of C=O and C−O, the addition of cellulose increased the hydrogen bonding of the hydrogel network, and the binding energy of C=O and C−O was greatly changed. N 1s is composed of one fitting group, with −NH$_2$ and 399.68 eV as the center. The binding energy of N−H hardly changed in

the three hydrogel samples, which indicates the stability of the formed amide groups.[41]

2.3. Poly(ethylene glycol)s of Different Molecular Weights Control the Structure and Performance of Starch−Acrylamide/Poly(ethylene Glycol) Hydrogels.

2.3.1. XRD (X-ray Diffraction) Patterns. Figure 4A shows the XRD patterns of hydrogels with different molecular weights. When the molecular weight of poly(ethylene glycol) was 200 (S-A/P200 in the figure), broad and weak peaks appeared at 2θ = 12, 23, and 42°. This shows the amorphous structure of the hydrogel.[42] Upon increasing the molecular weight of poly(ethylene glycol) (S-A/P400, S-A/P600, S-A/P800 in the figure), the peak at 12° disappeared, and the peak at 23° increased first and then weakened. The maximum peak value was obtained when the molecular weight was 600. There was almost no change in the peak at 42°. When the molecular weight of PEG is low, some of the small-molecule poly-(ethylene glycol) (PEG200) forms hydrogen bonds with starch molecules during the gel formation process. The other part fills in the network holes of the gel due to its low molecular weight to form a "microgel".[43] Microgels are micron-sized gel particles, which are polymer particles with an intramolecular cross-linked structure. Some small-molecule poly(ethylene glycols) form microgels during the formation of a hydrogel, and water acts as a good solvent for poly(ethylene glycol), which makes the volume of the formed microgels expand continuously and fill in the network cavities of the hydrogel; as the molecular weight of poly(ethylene glycol) increases, the effect of water as a solvent becomes less effective, leading to the structural collapse of the microgels.[44] Therefore, three amorphous peaks appeared when the molecular weight of poly(ethylene glycol) was low. As the molecular weight of poly(ethylene glycol) increased, the network pores cannot accommodate the microgel of larger molecules, so the amorphous peak at 12° disappears. The amorphous peak at 23° first increased and then decreased upon increasing the molecular weight of poly(ethylene glycol). As the molecular weight increased, the hydrogen bonding between poly-(ethylene glycol) and starch molecules increased, so the peak value increased, but when the molecular weight increased to a certain degree(S-A/P800), the fluidity of the molecular chain reduced, resulting in a decrease in the peak value.

2.3.2. Morphological Analysis. Figure 4B shows the topography of the cross-sectional structure of the prepared gel samples made with different molecular weights of poly(ethylene glycol). Figure 4a shows that the addition of low-molecular-weight poly(ethylene glycol) (PEG200) decreases the porosity of the hydrogel network, mainly because when the molecular weight of poly(ethylene glycol) is low, its molecular chain segments are too short to effectively overlap with long linear molecules. The poly(ethylene glycol) molecular chain itself or the starch molecular chain forms a microgel through the action of hydrogen bonds to fill the network pores of the hydrogel. As the molecular weight of poly(ethylene glycol) increased, the poly(ethylene glycol) molecules combined with the stretched amylose molecules through hydrogen bonds, so the network structure of the hydrogel slowly reformed, as shown in Figure 4b,c. Upon further increasing the molecular weight of poly(ethylene glycol), the molecular chains of poly(ethylene glycol) became too long, which reduced their fluidity and prevented them from forming more hydrogen bond cross-linking points with the amylose molecular chain; therefore, compared with the
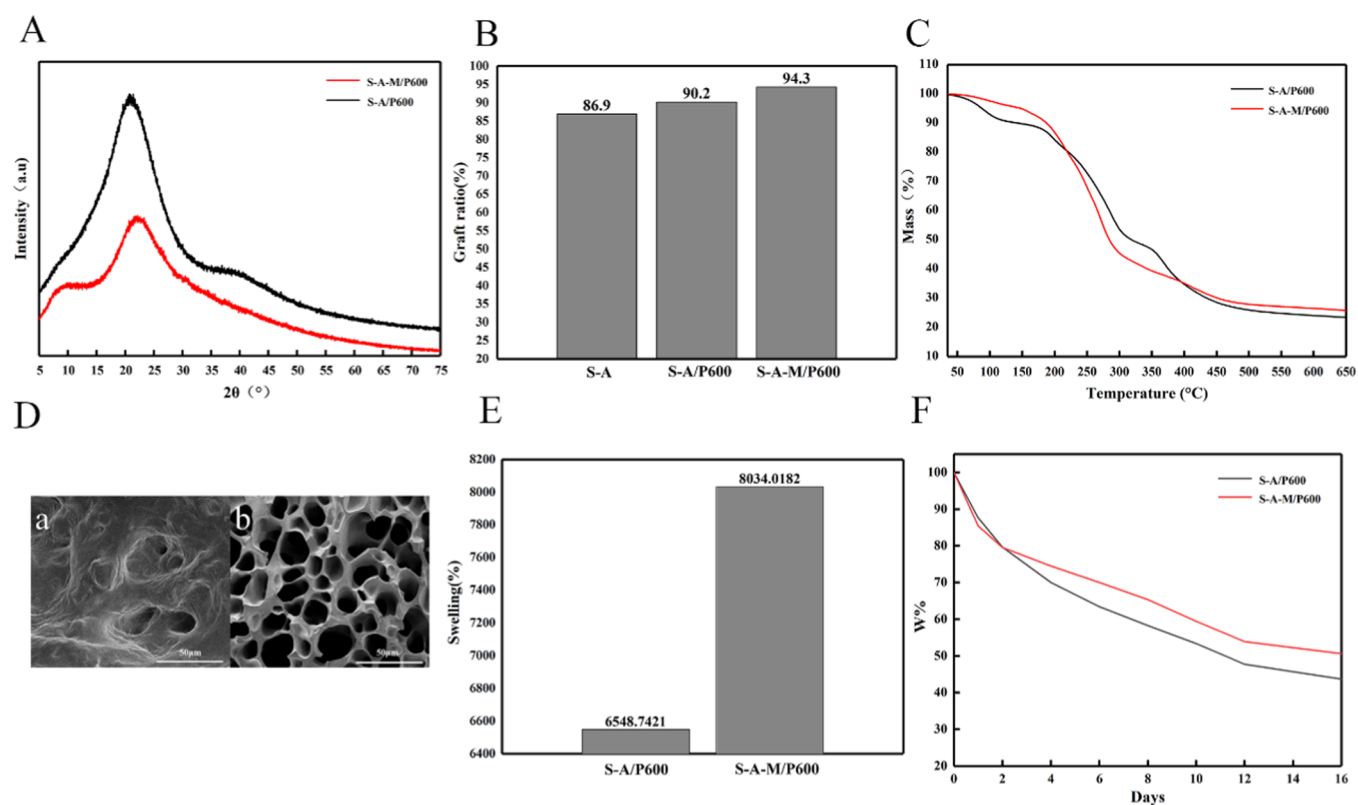
Figure 5. XRD patterns of S-A/P600 and S-A-M/P600 (A); grafting rate of S-A, S-A/P600, and S-A-M/P600 (B); thermogravimetric curve of S-A/P600 and S-A-M/P600 (C); SEM image of S-A-M/P600 (D); swelling performance of S-A/P600 and S-A-M/P600 (E); and 16 day water retention performance of S-A/P600 and S-A-M/P600 (F).

network structure of S-A/P600, the structure of S-A/P800 was less hollow.

2.3.3. Swelling Properties. Figure 4C shows the water swelling diagram of starch gels when blended with different molecular weights of poly(ethylene glycol). The water swelling ratio of the hydrogel samples first increased and then decreased upon increasing the molecular weight of poly(ethylene glycol). When the molecular weight of poly(ethylene glycol) was 600, the water swelling rate of the hydrogel reached the maximum (65.48 times). It is believed that the hydrogen bonds formed between poly(ethylene glycol) and starch provided more hydrophilic groups in the network structure of the sample, and the hydrogel is saturated at this time state. The hydrophilic −OH groups of poly(ethylene glycol) can absorb more water. When the molecular weight of poly(ethylene glycol) continues to increase, its molecular weight is too large, the mobility of the molecular chains is weakened, and many of its −OH groups become embedded in the molecular chain to form hydrogen bonds, decreasing their degrees of freedom and thus decreasing the hydrophilicity of the hydrogel.

2.3.4. Water Retention Performance. Figure 4D shows the 16 day water retention of poly(ethylene glycol) starch gels with different molecular weights. In the first 2 days, the free water absorbed by the gel sample evaporated quickly. As time passed, the bound water absorbed by poly(ethylene glycol) and the hydrophilic groups in the starch evaporated slowly. When the molecular weight of poly(ethylene glycol) was 600, the best water retention performance was obtained (16 day water retention rate was 45.67%). By comparing the experimental data, we found that the S-A hydrogel displayed the best water absorption and water retention when poly(ethylene glycol)

with a molecular weight of 600 was added; therefore, the experimental materials used in Section 2.3 are all S-A/P600.

2.4. Structure and Properties of the Starch−Acrylamide−Cellulose/Poly(ethylene glycol) Hydrogel.
2.4.1. XRD Patterns. Figure 5A shows the wide-angle diffraction pattern of S-A/P600 and S-A-M/P600, which both display broad and weak peaks at $2\theta = 12, 23$, and $42°$, which indicates that the hydrogel sample was amorphous. In addition, the diffraction peak intensity of S-A-M/P600 was weaker than that of the S-A/P600 hydrogel sample. The addition of cellulose reduced the number of hydrogen bonds between poly(ethylene glycol) and starch. The FTIR spectrum analysis shows that both cellulose and starch underwent a grafting reaction with acrylamide, so the hydrogen bonds between starch, cellulose, and poly(ethylene glycol) were weakened, which weakened the peak at $24°$. The peak at $11.8°$ represents the intramolecular hydrogen bond of the C6 atom on the (110) plane of microcrystalline cellulose. Its appearance proves the integrity of the cellulose structure, i.e., during hydrogel formation, some of the hydrogen bonds between the cellulose molecular chains still existed.

2.4.2. Grafting Rate. Figure 5B shows the grafting rates of the starch−acrylamide hydrogel (S-A), starch−acrylamide/poly(ethylene glycol) hydrogel (S-A/P600), and starch−acrylamide−cellulose/poly(ethylene glycol) (S-A-M/P600). Compared with S-A and S-A/P600, S-A-M/P600 has a very high grafting rate (94.3%), which was confirmed by the emergence of new peaks in the infrared spectrum. During the hydrogel formation, acrylamide was not only grafted. On the starch molecular chain, excessive initiators and cross-linking agents caused some of the acrylamide and cellulose molecules
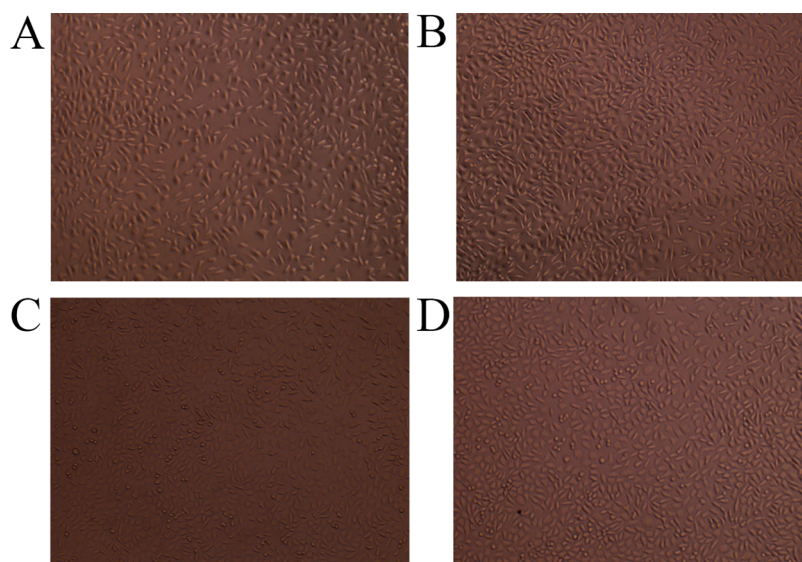
Figure 6. Photographs under the electron microscope of cell activity in blank samples (A, B) and the photographs under the electron microscope of cell activity in hydrogel extracts (C, D).

to undergo a grafting reaction,[45] which increased the grafting rate.

2.4.3. Thermal Stability. Figure 5C shows the thermal degradation curves of the starch−acrylamide/poly(ethylene glycol) hydrogel (S-A/600) and the starch−acrylamide−cellulose/poly(ethylene glycol) hydrogel (S-A-M/P600). The degradation curves can be roughly divided into four stages: 50−100, 150−300, 300−400, and 400−450 °C. Comparing the two degradation curves, the S-A-M/P600 hydrogel sample had a longer weight loss peak range from 300−400 °C. Therefore, the addition of cellulose improves the thermal stability of the hydrogel network.

2.4.4. Micromorphology Analysis. Figure 5D shows the surface (a) and cross-section (b) of the starch−acrylamide−cellulose/poly(ethylene glycol) hydrogel. The surface of S-A-M/P600 was relatively smooth, but it also contained micropores. This was mainly because microcrystalline cellulose contains many active hydroxyl groups that can participate in the polymerization and construction of a three-dimensional polymer network; therefore, the entanglement of the polymer chains and hydrogen bonds between hydrophilic groups can be prevented. This decreases the degree of physical cross-linking, which causes the rough surface of the hydrogel to become smoother in the presence of microcrystalline cellulose.[46] It can be seen from the cross-sectional view of the hydrogel that the prepared hydrogel formed a regular three-dimensional honeycomb-like network structure with a porous surface morphology. Analysis suggests that during the preparation of hydrogels, acrylamide is not only grafted onto the starch molecular chains but also onto the cellulose molecular chain. The cross-linking between acrylamide and starch and cellulose molecules formed a hydrogel. In addition, some of the starch and cellulose molecular chains that did not form chemical cross-links and poly(ethylene glycol) formed hydrogen bonds. This made the hydrogel network structure appear to have a synergistic effect between chemical cross-links and hydrogen bonds. The entire hydrogel network provided more cross-linking sites and strong support; therefore, the network pore size was reduced, the network pore walls thickened, and the network structure became more regular.

2.4.5. Swelling Properties. Figure 5E shows the water swelling diagram of the starch−acrylamide/poly(ethylene glycol) hydrogel (S-A/P600) and the starch−acrylamide−cellulose/poly(ethylene glycol) hydrogel (S-A-M/P600). The addition of rigid microcrystalline cellulose increased the water absorption performance of the hydrogel gel by 1.2 times (from 65.48 to 80.34 times). The addition of cellulose enhanced the ability of the hydrogel network structure to withstand damage and provided a stronger framework to support the network. It formed more hydrogel network voids, and the presence of poly(ethylene glycol) provided more hydrophilic groups, which allowed the hydrogel to entrain more water, thus greatly increasing its water absorption performance.

2.4.6. Water Retention Performance. Figure 5F shows the 16 day water retention curves of starch−acrylamide/poly-(ethylene glycol) (S-A/P600) and starch−acrylamide−cellulose/poly(ethylene glycol) (S-A-M/P600). In the first 2 days, the water loss rate of S-A-M/P600 was faster than that of S-A/P600. This analysis suggests that the initial water loss was mainly the free water contained in the hydrogel network. S-A-M/P600, which has a better water absorption effect, contains more free water, so its water loss rate is faster. As time passes, the subsequent water loss mainly comes from the bound water absorbed by the hydrophilic groups of poly(ethylene glycol) and the bound water in the starch−cellulose network. The addition of poly(ethylene glycol) provided more hydrophilic groups for the hydrogel so that the hydrogel can absorb and fix more water. The addition of cellulose improves the regularity of the hydrogel structure and enables the network structure of the hydrogel to lock more water, which greatly enhances the water retention capacity of the hydrogel. Meanwhile, cellulose itself is a hydrophilic material, and the addition of cellulose improves the hydrogel's water absorption capacity. Thus, the addition of microcrystalline cellulose and poly(ethylene glycol) greatly improved the water retention properties of the hydrogels. By comparing the experimental results, the water retention performance of S-A-M/P600 is better than that of some fertilizer-encapsulated materials.[47]

2.4.7. Cytotoxicity Testing of Hydrogels. The biocompatibility of hydrogel materials is an important criterion for the
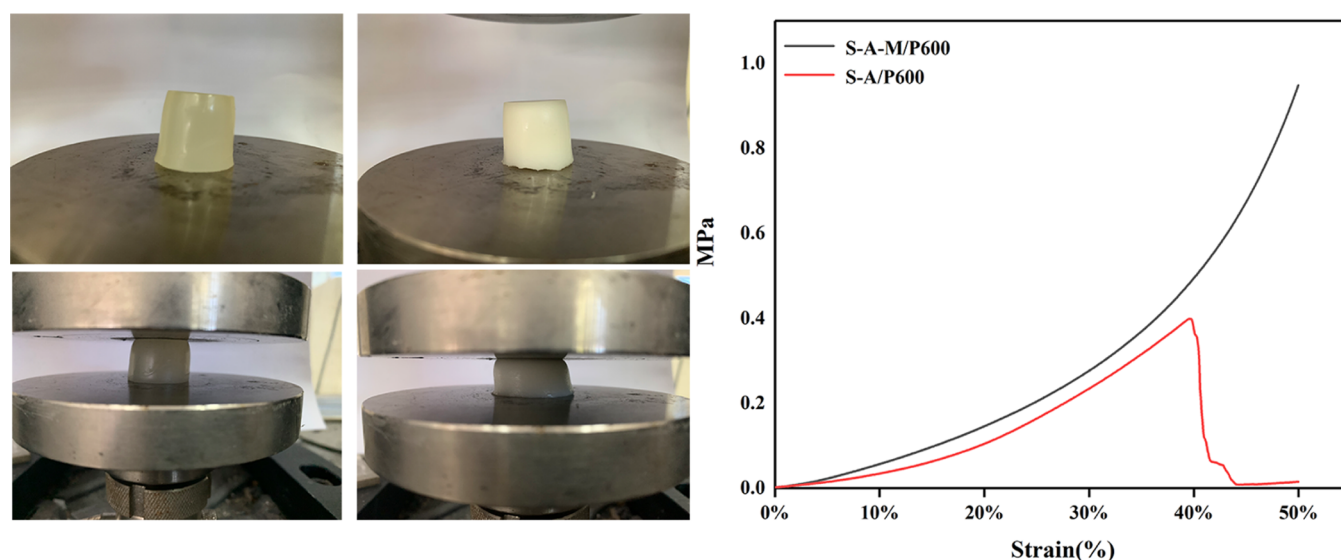
Figure 7. Compressive strength of S-A/P600 and S-A-M/P600.

widespread use of hydrogels. We have investigated the cytotoxicity of hydrogels by means of cell culture in hydrogel extracts. By comparing the cell survival rates of A and B in Figure 6, we can see that the number of cell death is small and the cell survival rate is high. We calculated by the formula that the cell viability value is around 89%. The experiment proves that the hydrogel material has very little toxicity to the cells, has good biocompatibility, and is suitable for water-absorbent materials.

2.4.8. Compression Stress−Strain Behavior of Hydrogels. We conducted compression performance tests on two types of hydrogels, S-A-M/P600 and S-A/P600. It was found that the compression performance of S-A-M/P600 was significantly better than that of S-A/P600. S-A/P600 exhibits a maximum compressive strength of 0.3992 MPa at a compressive strain of 39.85% (Figure 7). S -A-M/P600 was still not damaged when the compressive strain reached 50%, and the withstanding compressive strength could reach 0.9484 MPa. Through the experimental results, it can be found that the mechanical strength of the hydrogel was greatly improved by the addition of microcrystalline cellulose.[48]

The mechanical properties of this hydrogel exceed those of general starch hydrogels.[49]

3. CONCLUSIONS

In this paper, a superabsorbent hydrogel composite based on St-Mcc-graft-poly (AM) was prepared in the presence of APS as an initiator, MBA as a cross-linking agent, and MCC/PEG as an additive. FTIR results affirmed the occurrence of a grafting reaction between AM monomers and starch and the microcrystalline cellulose backbone, as well as the successful formation of the semi-IPN superabsorbent composite. As confirmed by SEM images, swelling properties, and water retention, cellulose was added as a rigid molecular chain to improve the water retention capacity and mechanical strength of the hydrogel; a superabsorbent and water-retaining hydrogel was prepared, which displayed a regular network structure that did not easily collapse. XRD analysis was used for further examination of the structural properties of the materials. The thermal stability of the material was studied by TG analysis. It is proved that the addition of cellulose improves the thermal

stability of the hydrogel. Poly(ethylene glycol) was added to a starch hydrogel to improve its water absorption capacity. Cellulose was added as a rigid molecular chain to improve the water retention capacity and mechanical strength of the hydrogel. A superabsorbent and a water-retaining hydrogel was prepared, which displayed a regular network structure that did not easily collapse. The poly(ethylene glycol) molecular chains contained abundant hydrophilic groups, so the hydrogels with added poly(ethylene glycol) showed good water absorption performance. Among them, poly(ethylene glycol) with a molecular weight of 600 displayed the most obvious improvement in the water absorption and water retention of hydrogels (the water absorption effect was 65.48 times, and the water retention rate at 16 days was 45.67%). The addition of microcrystalline cellulose increased the regularity of the hydrogel network structure, preventing it from easily collapsing, which greatly improved its water absorption and retention. The experimental results showed that the water absorption performance of the hydrogel was as high as 80.34 times. The water retention rate reached 50.61% at 16 days. The hydrogel structure was formed via synergistic effects between hydrogen bonds and chemical cross-links. Compared with general biopolysaccharide hydrogels, the compressive strength of the S-A-M/P600 hydrogel can reach 0.9484 MPa, and its mechanical properties far exceed those of most biopolysaccharide hydrogels.

Meanwhile, the cell survival rate of S-A-M/P600 can reach 89% in cytotoxicity assay, and this excellent biocompatibility cannot be achieved by general chemical hydrogels. According to the abovementioned results, the S-A-M/P600 hydrogel solves the problems of weak mechanical properties of general polysaccharide hydrogels and biotoxicity of chemical hydrogels, taking into account the excellent water absorption and retention properties, degradable properties, mechanical properties, and biocompatibility, and is a green water absorption material with application value and development potential.

4. MATERIALS AND METHODS

4.1. Materials. Starch (99% purity, Cool Bioengineering Co., Ltd. (Anhui, China)), *N,N*′-methylene bisacrylamide (MBA, AR, 99%, Aladdin, Shanghai, China), acrylamide (AM,

AR, 99%, Aladdin, Shanghai, China), cerium ammonium nitrate (AR, 99%, Sinopharm Chemical Reagent Co., Ltd.), sodium hydroxide (AR, 96%, Yongda Chemical Reagent Co., Ltd. (Tianjin, China)), poly(ethylene glycol) (PEG200, PEG400, PEG600, PEG800, Tianjin Komiou Chemical Reagent Co., Ltd.), microcrystalline cellulose (MCC, Mw (162.02))n, (Cool Bioengineering Co., Ltd., Anhui, China), and urea (AR, 99%, Aladdin Shanghai) were purchased from the respective companies.

4.2. Preparation of the Hydrogel. Overall, 3 g of poly(ethylene glycols) with different molecular weights (200, 400, 600, 800 g/mol) was placed in a 20 ml sample bottle. To melt the poly(ethylene glycol) to make it easier to mix with starch, the weighed sample bottles containing poly(ethylene glycol) were placed in a 60 °C water bath. The starch undergoes a pasting reaction at 60−65 °C. An appropriate amount of the starch mixture was placed into the other four sample bottles, acrylamide was added to each sample bottle, and the starch and acrylamide were mixed thoroughly using ultrasonication and mechanical stirring. Then, 0.1 g of N,N′-methylene bisacrylamide as a cross-linking agent was added to the sample bottle, followed by ultrasonic stirring for 10 min at 60 °C. After the temperature stabilized, the sample bottle was placed in an ultrasonic bath and stirred for 10 min. Then, poly(ethylene glycol) with different molecular weights was added to the sample bottles and reacted for 5 min under ultrasonic conditions. Then, an appropriate amount of a cerium ammonium nitrate solution was added to each sample bottle and reacted for 2 h. Then, a certain concentration of a sodium hydroxide solution was added, and the reaction was continued for 1 h. The hydrogel obtained after the reaction was repeatedly washed with distilled water, and the mixture was allowed to stand and swell for 6 h to completely dissolve unreacted substances. Finally, the hydrogel was obtained. The hydrogels containing different molecular weights of poly-(ethylene glycols) were named S-A /P200, S-A /P400, S-A /P600, and S-A /P800, and the hydrogel sample without poly(ethylene glycol) was named S-A.

Using Zhang et al.'s[50] cellulose dissolution method, a certain amount of cellulose was added to the prepared mixed solution of NaOH, urea, and deionized water. The ratio of sodium hydroxide:urea:water was 7:12:81. This mixture was mechanically stirred for 3 min and then put in a −15 °C refrigerator for 5 min until the mixed solution was completely clear. Then, it was removed for later use.

The next experimental steps are the same as above, except an appropriate amount of a microcrystalline cellulose solution was added before adding the cerium ammonium nitrate solution. The mixture was uniformly mixed through ultrasonic and mechanical stirring. The uniformly mixed solution was placed in an ultrasonic heating instrument at 60 °C for 5 min to remove air bubbles. Then, the prepared cerium ammonium nitrate solution was added to the mixture and reacted for 30 min. Finally, a certain amount of a sodium hydroxide solution was added, and the reaction was continued for 10 min. After the product was repeatedly washed with distilled water, it was allowed to stand and swell for 6 h in distilled water to completely dissolve unreacted substances. Then, it was repeatedly washed with additional distilled water. The final product starch−acrylamide−cellulose/poly(ethylene glycol) hydrogel was obtained, which was named S-A-M/P600.

4.3. Characterization of Hydrogels. A Fourier transform infrared spectrometer (NEXUS6700, Thermo Company) was used to characterize the functional groups of the hydrogel using potassium bromide tablets. The scanning wavenumber range was 500−4000 cm^{-1}.

X-ray photoelectron spectroscopy (XPS) was conducted on a Thermo Scientific K-α (Thermo Company) spectrometer equipped with a monochromatic Al Kα X-ray source (1486.6 eV) operating at 100 W. Samples were analyzed under vacuum ($P < 10^{-8}$ mbar) with a pass energy of 150 eV (survey scans) or 50 eV (high-resolution scans). All peaks would be calibrated with C1s peak binding energy at 284.8 eV for adventitious carbon.

X-ray diffraction analysis (Xpert Pro MPD, PANalytical, The Netherlands) was used to analyze the crystallinity of the gels. Cu Kα was used as a radiation source, and the test conditions are a tube current of 100 mA, a tube pressure of 40 kV, a step length of $2\theta = 0.02°$, and a 2θ range of 5−75°.

The grafting efficiency is often used to evaluate the degree of grafting copolymerization reactions and is typically performed by a mass analysis method. The crude product was weighed and wrapped in filter paper, then placed in a mixed solution of ethylene glycol and glacial acetic acid in a volume ratio of 6:4, followed by extraction for 24 h to remove the homopolymerization product. The product was then washed with ethanol and dried in a vacuum to a constant weight. The calculation formula is as follows

$$G = \frac{W_2}{W_1} \times 100\%$$

In the formula, G is the grafting rate of the gel, W_1 is the weight of the crude product (g), and W_2 is the weight of the refined product (g).

A PerkinElmer Diamond TGA system (Waltham, Massachusetts) was used to analyze the thermal decomposition of the gel. The measurement was performed by heating the sample from 35 to 650 °C at 10 °C/min under a nitrogen atmosphere and holding at 650 °C for 1 min.

A scanning electron microscope (JSM-7500F, JEOL, Japan) was used to observe the micromorphology of the hydrogels. All samples were sprayed with gold before analysis.

The water swelling rate was measured by the method of Xiao et al.[51] Specifically, 1 g of a dried sample gel was put into a bag and then immersed in distilled water for 6 h at ambient temperature. After that, the sample bag was hanged until no water dripped. Then, it was wiped with absorbent paper towels to remove free water. The net weight of each sample gel was determined. The water swelling rate (S) was calculated using the following equation

$$S(g/g) = \frac{(M_1 - M_2)}{M_2} \times 100\%$$

where $M1$ (g) and $M2$ (g) are the weights of the swollen and dried samples, respectively. All results were calculated as the average of three replicates.

To study the water retention of the sample hydrogel, the method of Olad et al.[52] was used. A gel sample was placed in a plastic cup with 100 g of dry loam (below 20 mesh). After that, 50 mL of distilled water was poured into a plastic cup, and it was weighed (W_0). The plastic cup was held at room temperature and weighed daily (Wt) for 16 days. Finally, the soil water retention rate (W) was determined by the following equation

$$W = \frac{W_t - W}{W_0 - W} \times 100\%$$

The appropriate amount of hydrogel samples was completely immersed in the medium according to ISO-10993 according to the standard of 0.2 g sample/ml and placed in a 37 °C environment, and the extracts of hydrogel samples were obtained after 72 h. Mouse epithelial-like fibroblast cells (L929) were inoculated into 24-well plates at a density of 10 000 cells per well and cultured in the medium for 24 h. The cells were then transferred to the medium containing the hydrogel extract and continued to be cultured for 48 h. Overall, 10 μL of a CCK-8 reagent was added to each well, and then the cells were continued to be incubated in a cell incubator at 37 °C for 1.5 h. The absorbance was measured at 450 nm using an enzyme marker. The pure medium without hydrogel extract was used as a blank control group, and each group contained four parallel samples. The calculation of cell viability was carried out by the formula, and the final results of the cytotoxicity test were obtained.[53,54] The cellular activity was determined by the following equation

Cellular activity(%) = $[(A1 - A2)/(A3/A2)] \times 100$

A1: The absorbance of the cell, CCK-8 solution, and drug solution. A2: The absorbance of the culture medium and the CCK-8 solution, without the cell. A3: The absorbance of cells and CCK-8 solution, without hydrogel extracts.

Mechanical properties of the composite hydrogel were analyzed by electronic universal (TSE-104B, Huaxing Company China).

AUTHOR INFORMATION

Corresponding Author

    Yuzhu Xiong − *Department of Polymer Materials and Engineering, Guizhou University, Guiyang 550025, P. R. China;* ⦿ orcid.org/0000-0001-6934-2672; Email: xyzhu789@126.com

Authors

    Longfei Gao − *Department of Polymer Materials and Engineering, Guizhou University, Guiyang 550025, P. R. China*

    Huiyuan Luo − *Department of Polymer Materials and Engineering, Guizhou University, Guiyang 550025, P. R. China*

    Qian Wang − *Department of Polymer Materials and Engineering, Guizhou University, Guiyang 550025, P. R. China*

    Guirong Hu − *Department of Polymer Materials and Engineering, Guizhou University, Guiyang 550025, P. R. China*

Complete contact information is available at:
https://pubs.acs.org/10.1021/acsomega.1c05614

Author Contributions

This manuscript was written through contributions of all authors. All authors have given approval to the final version of the manuscript.

Notes

The authors declare no competing financial interest.

REFERENCES

(1) Cassardo, C.; Tartaglia, A.; Mele, C.; Ruggiero, M. L. Global warming and water sustainability. *J. E3S Web Conf.* **2014**, *2*, No. 02006.

(2) Araújo, B. R.; Romao, L. P. C.; Doumer, M. E.; Mangrich, A. S. Evaluation of the interactions between chitosan and humics in media for the controlled release of nitrogen fertilizer. *J. Environ. Manage.* **2017**, *190*, 122−131.

(3) Wen, P.; Han, Y.; Wu, Z.; He, Y.; Ye, B. C.; Wang, J. Rapid synthesis of a corncob-based semi-interpenetrating polymer network slow-release nitrogen fertilizer by microwave irradiation to control water and nutrient losses. *Arabian J. Chem.* **2017**, *10*, 922−934.

(4) An, D.; Liu, B.; Yang, L.; Wang, T. J.; Kan, C. Fabrication of graphene oxide/polymer latex composite film coated on KNO_3 fertilizer to extend its release duration. *Chem. Eng. J.* **2016**, *311*, 318−325.

(5) Xiao, X.; Yu, L.; Xie, F.; Bao, X.; Liu, H.; Ji, Z.; Chen, L. One-step method to prepare starch-based superabsorbent polymer for slow release of fertilizer. *Chem. Eng. J.* **2017**, *309*, 607−616.

(6) Seetapan, N.; Wongsawaeng, J.; Kiatkamjornwong, S. Gel strength and swelling of acrylamide-protic acid superabsorbent copolymers. *Polym. Adv. Technol.* **2011**, *22*, 1685−1695.

(7) Zohuriaan-Mehr, M. J.; Kabiri, K. Superabsorbent Polymer Materials: A Review. *Iran. Polym. J.* **2008**, *17*, 451−447.

(8) Zohuriaan-Mehr, M. J.; Omidian, H.; Doroudiani, S.; Kabiri, K. Advances in non-hygienic applications of superabsorbent hydrogel materials. *J. Mater. Sci.* **2010**, *45*, 5711−5735.

(9) Zhang, J.; Wang, Q.; Wang, A. Synthesis and characterization of chitosan-g-poly (acrylic acid)/attapulgite superabsorbent composites. *Carbohydr. Polym.* **2007**, *68*, 367−374.

(10) Cipriano, B. H.; Banik, S. J.; Sharma, R.; Rumore, D.; Hwang, W.; Briber, R. M.; et al. Superabsorbent Hydrogels That Are Robust and Highly Stretchable. *J. Macromolecules* **2014**, *47*, 4445−4452.

(11) Kiatkamjornwong, S.; Mongkolsawat, K.; Sonsuk, M. Synthesis and property characterization of cassava starch grafted poly [acrylamide-co- (maleic acid)] superabsorbent viaγ-irradiation. *Polymer* **2002**, *43*, 3915−3924.

(12) Biduski, B.; da Silva, W. M. F.; Colussi, R.; El Halal, S. L.-M.; Loong-Tak, L.; Guerra Dias, A. R.; Zavareze, E. R. Starch hydrogels: The influence of the amylose content and gelatinization method. *Int. J. Biol. Macromol.* **2018**, *113*, 443−449.

(13) Chan, A. W.; Whitneym, R. A.; Neufeld, R. J. Semisynthesis of a controlled stimuli-responsive alginate hydrogel. *Biomacromolecules* **2009**, *10*, 609−616.

(14) Gattás-Asfura, K. M.; Weisman, E.; Andreopoulos, F. M.; Micic, M.; Muller, B. M.; Sirpal, S.; Pham, S. M.; Leblanc, R. Nitro-cinnamate-functionalized gelatin: Synthesis and "smart" hydrogel formation via photo-cross-linking. *Biomacromolecules* **2005**, *6*, 1503−1509.

(15) Xin, L.; Xu, S.; Yang, P.; Wang, J. The swelling behaviors and network parameters of cationic starch- g -acrylic acid/poly (dimethyldiallylammonium chloride) semi-interpenetrating polymer networks hydrogels. *J.Appl. Polym. Sci.* **2010**, *110*, 1828−1836.

(16) Ismail, H.; Irani, M.; Ahmad, Z. Starch-Based Hydrogels: Present Status and Applications: International Journal of Polymeric Materials and Polymeric Biomaterials: Vol 62, No 7. *Int. J. Polym. Mater.* **2013**, *62*, 411−420.

(17) Gombotz, W. R.; Wee, S. F. Protein release from alginate matrices. *Adv Drug Delivery Rev.* **2012**, *64*, 194−205.

(18) Sakeer, K.; Scorza, T.; Romero, H.; Ispas-Szabo, P.; Mateescu, M. A. Starch materials as biocompatible supports and procedure for fast separation of macrophages. *Carbohydr. Polym.* **2017**, *163*, 108.

(19) Thakur, V. K.; Thakur, M. K. Handbook of Polymers for Pharmaceutical Technologies. *Structure and Chemistry || Pharmaceutical Natural Polymers: Structure and Chemistry*, 2015; pp 477−519.

(20) Luo, L.; Gan, L.; Liu, Y.; Tian, W.; Tong, Z.; Wang, X.; Huselstein, C.; Chen, Y. Construction of nerve guide conduits from cellulose/soy protein composite membranes combined with Schwann cells and pyrroloquinoline quinone for the repair of peripheral nerve defect. *Biochem. Biophys. Res. Commun.* 2015, 457, 507−513.

(21) Ma, Z.; Li, Q.; Yue, Q.; Gao, B.; Xing, X.; Zhong, Q. Synthesis and Characterization of a Novel Super-Absorbent Based on Wheat Straw. *Bioresour. Technol.* 2011, 102, 2853−2858.

(22) Chang, C.; Duan, B.; Cai, J.; Zhang, L. Superabsorbent Hydrogels Based on Cellulose for Smart Swelling and Controllable Delivery. *Eur. Polym. J.* 2010, 46, 92−100.

(23) Zhang, Y. N.; Cui, J. Y.; Xu, S. A. Effects of chain Structures of Corn Starches on Starch-Based Superabsorbent Polymers. *Starch - Stärke* 2015, 67, 949−957.

(24) Zohuriaan-Mehr, M. J.; Kabiri, K. Superabsorbent Polymer Materials: A Review. *Iran. Polym. J.* 2008, 17, 451−447.

(25) Zohuriaan-Mehr, M. J.; Omidian, H.; Doroudiani, S.; Kabiri, K. Advances in non-hygienic applications of superabsorbent hydrogel materials. *J. Mater. Sci.* 2010, 45, 5711−5735.

(26) Ismail, H.; Irani, M.; Ahmad, Z. Starch-Based Hydrogels: Present Status and Applications. *Int. J. Polym. Mater.* 2013, 62, 411−420.

(27) Ullah, F.; Othman, M. B. H.; Javed, F.; Ahmad, Z.; Akil, H. M. Classification, processing and application of hydrogels: A review. *J. Mater. Sci. Eng., C* 2015, 57, 414−433.

(28) Campos, E. V. R.; Oliveira, De J. L.; Fraceto, L. F.; Singh, B. Polysaccharides as safer release systems for agrochemicals. *Agron. Sustainable Dev.* 2015, 35, 47−66.

(29) Coutinho, D. F.; Sant, S. V.; Shin, H.; Oliveira, J. T.; Gomes, M. E.; Neves, N. M.; Khademhosseini, A.; Rui, L. R. Modified Gellan Gum hydrogels with tunable physical and mechanical properties. *Biomaterials* 2010, 31, 7494−7502.

(30) Guo, Y.; Bae, J.; Fang, Z.; Li, P.; Yu, G.; et al. Hydrogels and Hydrogel-Derived Materials for Energy and Water Sustainability. *J. Chem. Rev.* 2020, 120, 7642−7707.

(31) Lund, D.; Lorenz, K. J. Influence of time, temperature, moisture, ingredients, and processing conditions on starch gelatinization. *CRC Crit. Rev. Food Sci. Nutr.* 1984, 20, 249−273.

(32) Lanthong, P.; Nuisin, R.; Kiatkamjornwong, S. Graft copolymerization, characterization, and degradation of cassava starch-g-acrylamide/itaconic acid superabsorbents. *Carbohydr. Polym.* 2006, 66, 229−245.

(33) Willett, J. L.; Finkenstadt, V. L. Preparation of starch-graft-polyacrylamide copolymers by reactive extrusion. *Polym. Eng. Sci.* 2003, 43, 1666−1674.

(34) Qiao, D.; Liu, H.; Yu, L.; Bao, X.; Simon, G. P.; Petinakis, E.; Chen, L. Preparation and characterization of slow-release fertilizer encapsulated by starch-based superabsorbent polymer. *Carbohydr. Polym.* 2016, 147, 146−154.

(35) Subramanian, K.; Dhanapal, V. Recycling of textile dye using double network polymer from sodium alginate and superabsorbent polymer. *Carbohydr. Polym.* 2014, 108, 65−74.

(36) Pandey, M.; Mohamad, N.; Amin, M. Bacterial Cellulose/Acrylamide pH-Sensitive Smart Hydrogel: Development, Characterization, and Toxicity Studies in ICR Mice Model. *Mol. Pharmaceutics* 2014, 11, 3596−3608.

(37) Tang, L.; Zhao, X.; Feng, C.; et al. Bacterial cellulose/MXene hybrid aerogels for photodriven shape-stabilized composite phase change materials. *Sol. Energy Mater. Sol. Cells* 2019, 203, No. 110174.

(38) Marandi, G. B.; Esfandiari, K.; Biranvand, F.; Babapour, M.; Sadeh, S.; Mahdavinia, G. R. pH Sensitivity and Swelling Behavior of Partially Hydrolyzed Formaldehyde -Crosslinked Poly (acrylamide) Superabsorbent Hydrogels. *J. Appl. Polym. Sci* 2008, 109, 1083−1092.

(39) Demeyer, P. J.; Bloemen, M.; Verbiest, T.; Clays, K. Tuning the properties of colloidal magneto photonic crystals by controlled infiltration with superparamagnetic magnetite nanoparticles. *J. Proc. SPIE.* 2012, 8425, 84251R.

(40) He, S.; Fan, Z.; Cheng, S. Synthesis of sodium acrylate and acrylamide copolymer/ GO hydrogels and their effective adsorption for Pb^{2+} and Cd^{2+}. *ACS Sustainable Chem. Eng.* 2016, 4, 3948−3959.

(41) Liu, H.; Wang, Q.; Zhang, F. Preparation of Fe3O4 @ SiO2@ P(AANa-co-AM) Composites and Their Adsorption for Pb (II). *ACS Omega* 2020, 5, 8816−8824.

(42) Olad, A.; Pourkhiyabi, M.; Gharekhani, H.; Doustdar, F. Semi-IPN superabsorbent nanocomposite based on sodium alginate and montmorillonite: Reaction parameters and swelling characteristics. *Carbohydr. Polym.* 2018, 190, 295−306.

(43) Coskun, M.; Temüz, M. M. Grafting studies onto cellulose by atom-transfer radical polymerization. *Polym. Int.* 2005, 54, 342−347.

(44) Saunders, B. R.; Vincent, B. Microgel particles as model colloids: theory, properties and applications. *Adv. Colloid Interface Sci.* 1999, 80, 1−25.

(45) Olad, A.; Doustdar, F.; Gharekhani, H. Fabrication and characterization of a starch-based superabsorbent hydrogel composite reinforced with cellulose nanocrystals from potato peel waste − ScienceDirect. *J. Colloids Surf, A.* 2020, 601, No. 124962.

(46) Lue, A.; Zhang, L.; Ruan, D. Inclusion Complex Formation of Cellulose in NaOH−Thiourea Aqueous System at Low Temperature. *Macromol. Chem. Phys.* 2007, 208, 2359−2366.

(47) Wang, Y.; Liu, M.; Ni, B.; Xie, L. κ-Carrageenan−Sodium Alginate Beads and Superabsorbent Coated Nitrogen Fertilizer with Slow-Release, Water-Retention, and Anticompaction Properties. *Ind. Eng. Chem. Res.* 2012, 51, 1413−1422.

(48) Zhu, B.; Ma, D.; Wang, J.; Zhang, S. Structure and properties of semi-interpenetrating network hydrogel based on starch. *Carbohydr. Polym.* 2015, 133, 448−455.

(49) Yang, J.; Chun Rui, H. Mechanically Viscoelastic Properties of Cellulose Nanocrystals Skeleton Reinforced Hierarchical Composite Hydrogels. *ACS Appl. Mater. Interfaces* 2016, 8, 25621−25630.

(50) Dong, R.; Lue Ang, A. L. Gelation behaviors of cellulose solution dissolved in aqueous NaOH/thiourea at low temperature. *Polymer* 2008, 49, 1027−1036.

(51) Xiao, X.; Yu, L.; Xie, F.; Bao, X.; Liu, H.; Ji, Z.; Chen, L. One-step method to prepare starch-based super absorbent polymer for slow release of fertilizer. *Chem. Eng. J.* 2017, 309, 607−616.

(52) Olad, A.; Zebhi, H.; Salari, D.; Mirmohseni, A.; Tabar, A. R. Slow-release NPK fertilizer encapsulated by carboxymethyl cellulose-based nanocomposite with the function of water retention in soil. *J. Mater. Sci. Eng. C* 2018, 90, 333−340.

(53) Xiao, D.; Zhang, Y.; Wang, R. Emodin alleviates cardiac fibrosis by suppressing activation of cardiac fibroblasts via upregulating metastasis associated protein 3. *Acta Pharm. Sin. B* 2019, 9, 724−733.

(54) Li, M.; Chen, J.; Yu, X.; et al. Myricetin Suppresses the Propagation of Hepatocellular Carcinoma via by Down-Regulating Expression of YAP. *Cells* 2019, 8, No. 358.